



Evaluating the strategy of integrated urban-rural planning system and analyzing its effects on land surface temperature in a rapidly developing region



Roshanak Afrakhteh^a, Ali Asgarian^b, Yousef Sakieh^c, Alireza Soffianian^{b,*}

^a Department of the Environmental Sciences, Faculty of Agriculture and Natural Resources, University of Hormozgan, Hormozgan, Iran

^b Department of Natural Resources, Isfahan University of Technology, Isfahan 84156-83111, Iran

^c College of the Environmental Sciences, Gorgan University of Agricultural Sciences and Natural Resources, Golestan, Iran

ARTICLE INFO

Article history:

Received 19 October 2015

Received in revised form

16 May 2016

Accepted 27 May 2016

Keywords:

Integrated urban-rural planning

Land surface temperature

Scenario-based urban growth modeling

CA-Markov model

Rural development

Iran

ABSTRACT

This study highlights the importance of integrated urban-rural land-use planning system in a rapidly developing region, Falavarjan Township, Iran. It also analyses the effect of various urban growth policies on land surface temperature (LST). In doing so, this paper combines several modeling methods including LST map generation algorithm, urbanization suitability mapping, and scenario-based analysis of future circumstances through cellular automata (CA)-Markov modeling and regression analyses. The potential impact of various urban growth policies including historical growth, extensive growth and rural development on LST values of interior urban environments are quantified and compared. These scenarios are introduced to the CA-Markov model by generating several urbanization suitability layers insisting on various urban-rural planning perspectives. In addition, linear, quadratic and logarithmic regression models were also developed to measure the relationship between LST values and urban patches areas. The results demonstrated that logarithmic regression model yields stronger relationships ($R^2 = 0.35$, $p < 0.01$) such that the model is capable of predicting LST values over temporal scales. By coupling the results derived from CA-Markov model and temporal estimation of LST values, an integrated urban-rural land-use planning system is developed. The findings of this study can effectively assist land managers in central Iran to adopt a sustainable planning strategy in a highly developing region.

© 2016 Elsevier Ltd. All rights reserved.

1. Introduction

The world has witnessed an unprecedented urbanization growth rate during the last century and this urbanization demonstrates no sign of slowing down (Alhowsaish, 2015; Jusuf, Wong, Hagen, Anggoro, & Hong, 2007). Urbanized lands are responsible for approximately 80% of carbon emissions, 60% of residential water consumption and almost 80% of wood utilized in industry (Schneider, Friedl, & Potere, 2010; Wu, 2010). The astonishing rate of growth in both human population and human-made constructions alarms on future environmental consequences originated from this rapid and sharp expansion (Douglas, Goode, Houck, & Wang, 2011; Niemelä et al., 2011).

One of the well-documented effects of urbanization is possibly the urban heat island (UHI) effect. Drastic changes on climatic conditions brought about by human activities affected urban sustainability by aggravating the conflict between water supply and demand, increasing energy use and rising flood risk (Hansen, 2010). Conversely, there is a loop feedback by which urban growth can similarly affect some meteorological parameters that can significantly alter regional climatic regimes (Gu, Hu, Zhang, Wang, & Guo, 2011; Wu, 2014). In this regard, several studies have reported that future land-use changes are inevitably correlated with modification of climatic conditions and urban landscape would undergo different situations in terms of various spatial policies and meteorological circumstances (He, Zhao, Huang, Zhang, & Zhang, 2015; Solomon, 2007). Therefore, evaluating the interrelated relationships between land-use pattern changes and climatic regimes can provide valuable insights on urban sustainability (Sánchez-Rodríguez, 2005; Wu & Wu, 2013). In this case, Land surface temperature (LST) has been an active topic of research during the last decade.

* Corresponding author.

E-mail addresses: Roshanak_afra@yahoo.com (R. Afrakhteh), asgarian.z@gmail.com (A. Asgarian), sakie.yusuf@gmail.com (Y. Sakieh), soffianian@cc.iut.ac.ir (A. Soffianian).

Majority of researches in this field adopted a static approach. These studies have basically been undertaken to examine the linkage between LST and land surface characteristics such as impervious surface (Bokaei, Zarkesh, Arasteh, Hosseini, 2016) and vegetative covers (Huang, Chen, Li, Shen, & Li, 2016), the size and spatial patterns of different land-use/covers (Zhou, Huang, & Cadenasso, 2011), neighbor cover types (Asgarian, Amiri, & Sakieh, 2014; Feng & Myint, 2016) and fraction variables (Amiri, Weng, Alimohammadi, & Alavipanah, 2009; Lu and Weng, 2005). Moreover, there is also a high number of studies dealing with the spatiotemporal variability of LST in relation to urban growth patterns and trajectories (Chaudhuri & Mishra, 2016; Du, Xiong, Wang, & Guo, 2016; Feng, Zhao, Chen, & Wu, 2014) and natural/open space land cover changes (Vlassova & Pérez-Cabello, 2016). In this regard, there are few studies focusing on temporal predictive ability of LST in dynamic landscapes. To our knowledge, only a limited number of researches such as He et al. (2015), Verburg, van Berkel, van Doorn, van Eupen, and van den Heiligenberg (2010) and Bryan, Crossman, King, and Meyer (2011) adopted an integrative approach by coupling system dynamics and land-use/cover change models to link climate change (not LST) to future land-use change trajectories.

The dynamic approach permits the modeler to examine the cumulative effects of urban growth policies on LST and also it allows comparing the effectiveness of various planning strategies over time (Feng et al. 2014). Generally, dynamic studies are inevitably multidisciplinary which necessitate integration of various databases from different sources. Moreover, dynamic studies rarely follow a holistic manner to compare and analyse the effect of multiple scenarios ranging from urban development plans to rural land management. The results of such study can provide an informed set of decisions and offers an interactive planning tool that systematically analyses a developing landscape. Therefore, rural and urban land enforcements can be wisely regulated that finally improve comprehensive urban sustainable development plants.

The present study adopts an integrative modeling approach and implements several modeling tools. In other words, the current paper couples scenario-based CA-Markov modeling, LST map generation algorithm, and statistical analyses to quantitatively explore the relationships between urban growth policies and LST values distribution across a developing landscape in Falavarjan Township, Iran. These modeling tools are mainly incorporated to answer the following questions:

- (1) What is the actual relationship (linear, quadratic or logarithmic) between area of built-up structures of various physical sizes in Falavarjan Township area and LST values distribution in interior urban environments?
- (2) In case of any relationship, do LST values can be predicted over temporal scales using built-up land area as an explanatory variable?
- (3) How both temporal LST prediction and predictive urban growth modeling can be coupled in an integrative geospatial study?
- (4) What is the appropriate growth policy for designing an urban landscape with lower levels of LST values?
- (5) How integrated urban-rural development plans can be adopted to design an urban landscape with lower LST values and appropriate connectivity and compactness of human-made elements?

2. Materials and methods

2.1. Study area

Falavarjan Township as a typical and representative case of urbanized landscape in central Iran was selected as the study area for this research (Fig. 1). Nearly 70 towns and villages in the south-west of Isfahan City border the Falavarjan Township, with a complete

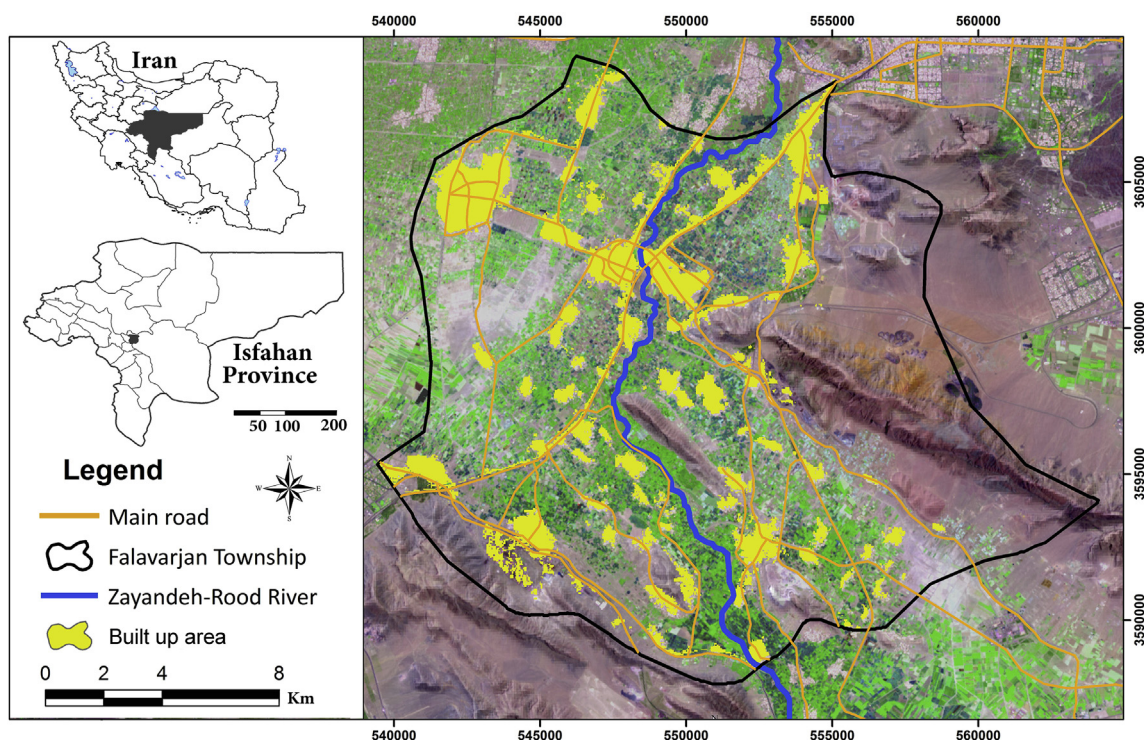


Fig. 1. Geographic location of the study area.

plain area of 324 km² (51.41–51.66 E and 32.40–32.61 N). Based on 2015 census data, Falavarjan is resided by more than 240,000 inhabitants accommodated in 8 urban centres and more than 55 small towns, accounting for 60% and 40% of total population, respectively. The population of the study area added 84,500 (0.25%) to its population since 2002 (from 191,500) and exceeded 200,000 by 2009.

The precipitation of the study area is annually less than 130 mm that mainly occurs in winter and early spring. The main source of water is from the snow-capped Zard-kooh Mt. that supplies water needs in the basin. The water runs through Zayandeh-rood seasonal river and traverses the entire basin, including 15 km inside the study area. Currently, land-use managers' retrospective efforts through rural development plans have thoroughly focused on preserving present landscape pattern which has been traditionally dominated by small towns and villages. These plans have been expected to preserve agricultural areas and finally to support ecological and economic advantage such as food security, ground water feeding, and maintaining multiple use of ecosystems services.

2.2. LST map generation

Landsat 7 ETM+ imagery over Isfahan Province, path 164 and row 37, was used as the main data to retrieve LST map. For selecting the appropriate imagery, in addition to image quality and cloud coverage control, the stability of some meteorological parameters for a specific period of time before image acquisition date was also considered. This is an important factor that affects the accuracy of LST map. In this respect, the Landsat 7 ETM+ image on May 5, 2002 (cloud coverage of 0.31%) was processed. Based on meteorological data obtained from three weather stations (distributed across the study area), the mean temperature on May 5, 2002 was 29.8 °C with evaporation and relative humidity of 12.4 mm and 3.4%, respectively.

LST retrieval involves three successive steps (Weng, Lu, & Schubring, 2004). In the first step, digital numbers (DNs) of Landsat TIR band were converted to spectral radiance. In the next step, spectral radiance was transformed to at-satellite brightness temperature (T_B). T_B or temperature (in kelvin) is referenced to black-bodies, ideal radiant materials, however, natural covers have the ability to reflect or/and transmit the specific amount of electromagnetic energy. Therefore, spectral emissivity (ϵ) values related to different land features were used to convert T_B to LST. In this case, The NDVI Threshold Method (Sobrino, Jiménez-Muñoz, & Paolini, 2004) was used to estimate spectral emissivity of different land surface types due to their electromagnetic reflectance. This method categorizes various land-use/cover types through a NDVI classification scheme to obtain land surface spectral emissivity. Finally, LST retrieval accuracy was assessed using in-situ soil surface temperature data acquired from three weather stations across the study area (at 9 a.m. local time). For a more detailed description and formulation of LST retrieval steps used in this work, readers are referred to Weng et al. (2004) and Sobrino et al. (2004).

2.3. Built-up land-use classification

Landsat tiles on June 2010 (TM 5 sensor) and 2014 (OLI 8 sensor) were also acquired (in addition 2002 image) to delineate built-up land-use. Digital topographic maps (2001) with scale of 1:25,000 were also used as auxiliary data for image processing. Besides, a large number of 1:200 printed maps of rural areas of the years 2002 and 2008 were also employed as reference data to support built-up land use classification process and validation.

Visual interpretation method was adopted for generating three

built-up map layers. Accordingly, using an appropriate three-band combination of the Landsat tiles, three 24-bit RGB images were created for each Landsat scene including a true/natural (RGB of 3,2,1) and two false colour composite images (RGB of 7,4,1 and 4,3,2). They were then printed with the scale of 1:100,000 for better visualization of the objects in 30 m spatial resolution. Meanwhile, built-up land polygons were digitized pixel by pixel on a computer screen to generate final built-up map layer. Although spending considerable time recognizing built-up polygons, the aforementioned method greatly helped us to derive a high accurate built-up map by eliminating the salt and pepper pixels that significantly affect the results. The classification accuracy of each built-up map was evaluated by calculating Kappa Coefficient and Overall Accuracy indices from confusion matrices.

2.4. Modeling the relationship between mean LST and spatial pattern of built-up lands

An attempt was made to quantify and analyse the relationship between LST values and the area of built-up patches in our study site. A series of regression analyses consisting of linear, logarithmic and quadratic transformed models were employed to model the statistical relationship between mean LST values within each built-up patch (dependent variable) and area of the urban patch. The regression equations are provided as follows [1–3]:

$$\text{Linear regression : } y_i = \beta_0 + \beta_1 x_i + \epsilon_i \quad (1)$$

$$\text{Quadratic regression : } y_i = \beta_0 + \beta_1 x_i^2 + \epsilon_i \quad (2)$$

$$\text{Logarithmic regression : } y_i = \beta_0 + \beta_1 \log x_i + \epsilon_i \quad (3)$$

where y_i is the dependent variable (LST), x_i refers to independent variable (area of built-up patches), $\hat{\alpha}_0$ is model's intercept and β_i indicates model's coefficients, ϵ_i stands for error variable.

In this study, in line with other studies such as (Tan & Li, 2015; Zhou, Rybski, & Kropp, 2013), the area of built-up lands has been considered as the main spatial metric affecting the LST distribution. Accordingly, a significant regression model (p -value, *adjusted* R^2) has properly been developed from the given data. As it will be mentioned, the model results were subsequently used to evaluate the future built-up and LST patterns under different land-use change scenarios.

To do so, it is important to evaluate if the proposed regression model could be applied in several consecutive years, i.e., modeling the relationship between mean LST and the area of built-up patches in time spans (years) and then investigating the stability of model parameters in that period of time. In this study, using LST data retrieved from the ETM + fine resolution thermal bands, a significant regression model was formed for 2002 (section 2.2). However, ETM + thermal bands have only been available for the time period between 1999 and 2003 (Aronoff, 2005) and therefore, to form the second regression model, LST map must be retrieved from thermal bands of the other Landsat systems, including TIRS or TM with spatial resolution of 100 and 120 m, respectively. In this case, due to the spatial scale mismatch problem, it is theoretically impossible to model the relationship between small built-up patches (50% of them are less than 10 ha) and the mean values of coarse resolution LST data.

As a way of using LST data (retrieved from Landsat-8 TIRS data) to form the second regression model, only 20 built-up patches in the study site with more than 35 ha of interior area were involved in the temporal validation of the models (one model for 2002 and one model for 2014). Due to the size and spatial structure, these 20

built-up patches are considered to be less affected by LST values of the urban fringe areas (LST of mixed pixels of urban and agriculture). Therefore, having the areas of these 20 built-up patches extracted from 2010 to 2014 land-use maps, 2002 and 2014 LST maps were retrieved from Landsat-8 TIRS sensor as a secondary data (from Data Archive of Isfahan Municipality, no: 5054992 (Isfahan Municipality, 2016)) and the statistical relationship between mean LST and the area of the aforementioned 20 built-up patches were assessed for the years 2002 and 2014. Finally, *t*-test statistical analysis was used in order to determine whether there is any significant and stable relationship between the variables in time spans.

2.5. Scenario-based urbanization suitability mapping and urban growth modeling

2.5.1. Urbanization suitability mapping through multi-criteria evaluation (MCE)

MCE is generally a raster-based computation procedure on multiple input layers that are assumed to significantly influence the suitability of the land for a specific use. In doing so, a collection of raster maps of various environmental factors and constraints are provided in which each layer includes cells with different values (based on different measurement levels). Therefore, using Boolean logic and fuzzy set theory (Zadeh, 1965), the maps could be standardized. Another method implemented in a MCE study is analytical hierarchy process (AHP) (Saaty, 1990). AHP specifies weights to the standardized factor maps according to matrix computations. Generally, the standardized layers are combined through Weighted Linear Combination (Eastman, 2009). In the MCE analysis of Falavarjan Township, a collection of 8 factor layers were included (Table 1). For introducing urban growth scenarios in the next step, three urbanization suitability maps were generated based on different weighting schema of factor layers. Referring to similar studies (Goodarzi, Sakieh, & Navardi, 2016; Sakieh, Amiri, Danekar, Fegghi, & Dezhkam, 2014a, 2014b; Sakieh et al. 2015; Sakieh & Salmanmahiny, 2016; Xiang & Clarke, 2003), the predictive scenarios were outlined as follows:

- (1) Historical Growth (HG): The HG scenario or 'business as usual' assumes that historical growth profile in the past is expected to continue in the future. Under such growth trajectory, urban patches of varying size will experience a similar growth rate and growth pattern as their corresponding time profile in the past.
- (2) Extensive Growth (EG): Under such pattern urban, growth rate will be accelerated. Based on EG scenario, adjacent lands

to urban boundaries will possess higher suitability values for urbanization. In other words, current urban patches of varying size will experience an outward form of expansion and linear growth will cause separated urban edges to grow together and form larger patches.

- (3) Rural development (RD): This form of growth allows the behaviour of decentralized urban growth allocation for the model. In other words, distant lands to current urban boundaries possess higher levels of urbanization suitability. Under such pattern, further sprawl of major urban cores that are possibly beyond their carrying capacity in terms of number of residents and ecological footprint are prohibited. Accordingly, a spotty arrangement of urban patches will be allocated, while these newly urbanized lands have a medium size and larger patches have already minimized their growth cycles.

These layers were used to introduce the predictive growth scenarios through the CA-Markov model. The following sections will describe how the model was implemented to incorporate suitability surfaces and to spatially project future urban land-use change under such scenarios.

2.5.2. CA-Markov model

The CA-Markov model is a multi-objective land allocation algorithm for prediction of land-use change that incorporates spatial dimension. As a central characteristic, the Markov model takes the quantity of required change into account. For such model, spatial dimension is implicit and land-use features are not explicitly modelled. Therefore, combined CA-Markov model has a strong capability to analyse dynamic evolutions within a complex spatial problem. In doing so, map layers of 2010 and 2014 were first employed for model performance evaluation. Having the calibrated model validated, the 2014 map layer was used for model prediction stage. These steps were repeated for three predictive scenarios in which each growth option utilized its own urbanization suitability layer in model prediction run (and not in model calibration). As a result, each growth storyline yielded its own temporal growth signature for 2020, 2025 and 2030.

2.6. Analysing the effect of predictive urban growth scenarios on LST values within urban interior environment

The relationships between various urban growth policies and urban patches temperatures were also studied. Based on the appropriate regressive model, LST values for urban patches of varying size and under various scenarios were predicted (for 2020,

Table 1
Criteria maps, fuzzification method and weighting score used in this study to generate urbanization suitability maps under three scenarios of HG (historical growth), EG (extensive growth) and rural development (RD).

	Criteria	Description	Function type	Control points				Scenario weights		
				a	b	c	d	HG	EG	RD
Factor	Main city	Distance from cities (m)	Decreasing S	—	—	500	2500	0.133	0.233	0.053
	Rural area	Distance from towns (m)	Decreasing S	—	—	300	1000	0.179	0.022	0.390
	Existing roads	Distance from main (asphalt) roads (m)	Inverted J	—	—	250	750	0.870	0.530	0.160
	Population	Population per city/rural	Rescaling	Scenario-based				0.152	0.247	0.590
	Township center	Distance from Falavarjan city (m)	Decreasing L	Scenario-based				0.139	0.185	0.042
	Zobahan highway	Distance from the main road in the study area (m)	Inverted J	—	—	500	1500	0.074	0.093	0.066
	Industrial spots	Distance from industrial area (m)	Decreasing L	—	—	0	10,000	0.138	0.121	0.127
	North-easting coordination	Distance from Isfahan city and recreational areas (m)	Decreasing L	—	—	0	10,000	0.980	0.047	0.103
	Consistency ratio							0.066	0.083	0.054
Constraint	Slope	In order to exclude the mountainous areas	Boolean							
	River	200 m buffer zone of Zayandeh-rood river	Boolean							
	Arable Lands	Existing high quality agricultural areas (two crop rotation in a year)	Boolean							

2025 and 2030). For each node year and under each scenario, the number of urban patches with LST values above 40 °C was counted. The choice of 40 °C is based on study by (FMS., 2002), which reports that carrying capacity of the most residents against excessive temperatures cannot exceed 40 °C in Isfahan residential areas. Therefore, number of urban patches with LST values below this threshold can serve as an indicator for sustainability of a growth scenario in terms of providing cooler cities. Fig. 2 demonstrates the main steps undertaken in this study.

3. Results

3.1. Satellite image processing and LST map generation

Built-up maps of the years 2002, 2010, and 2014 have precisely been derived from Landsat tiles by employing a visual interpretation method (Fig. 3a, b, and 3c). Tables 2 and 3 provide information on classification accuracy assessment as well as satellite data used and the derived results in this step. Based on results obtained from

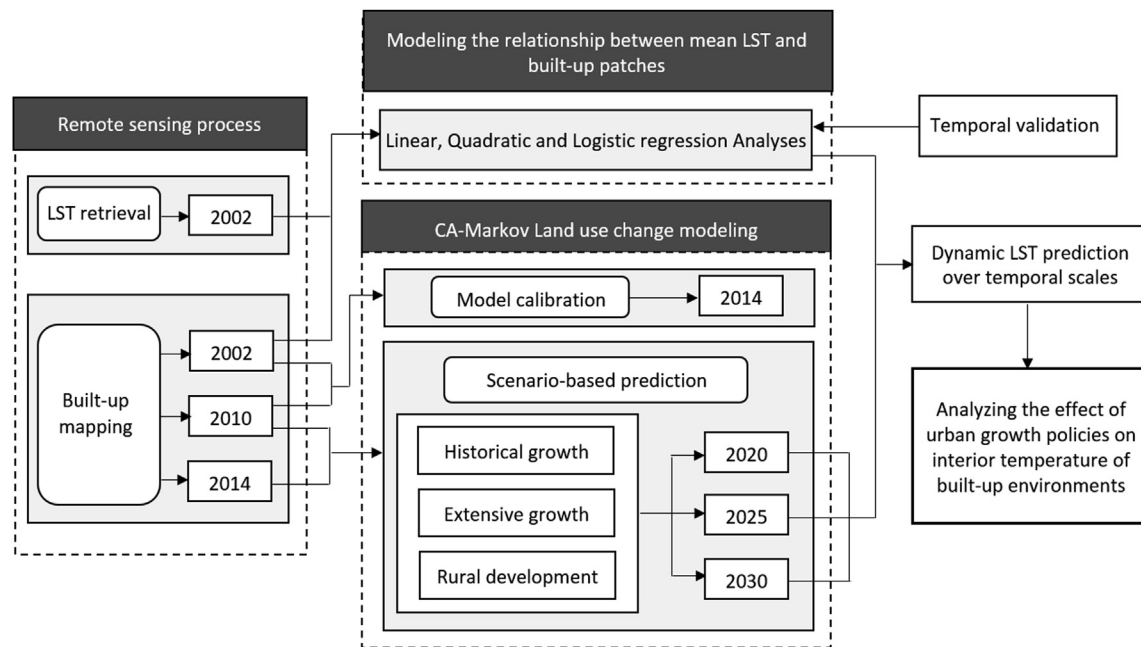


Fig. 2. Flowchart of the methodology.

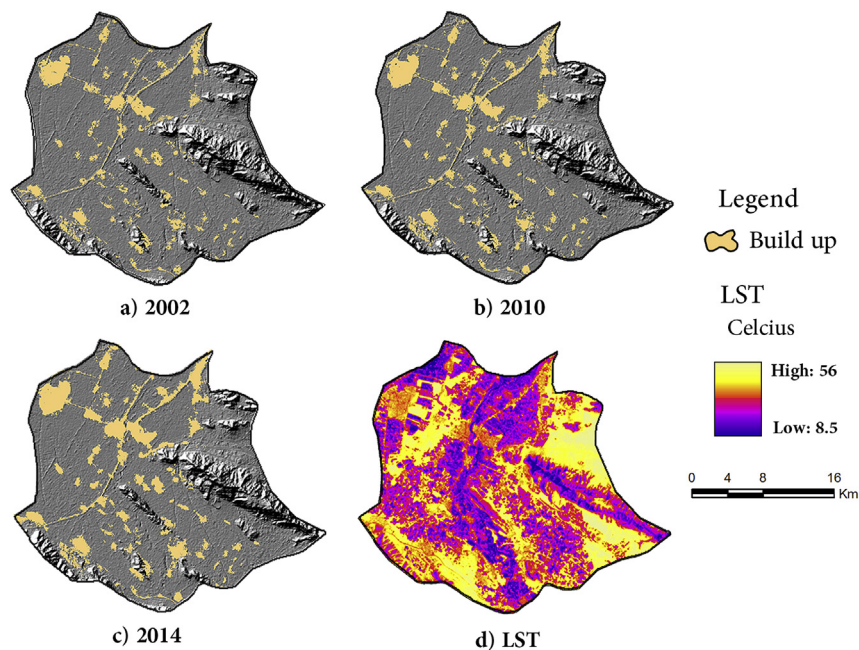


Fig. 3. LST and historical built-up maps of the study resulted from image processing.

Table 2
Statistical summary of classification accuracy assessment.

year	Reference points		year	Number of reference points	Accuracy statistics	
	Data type	source			Kappa Coefficient	Overall Accuracy
2002	GPS field-collected points	Field investigations	2001	617	85	90
2010	1:25000 digital topographic map	National Cartographic Center	2009	775	88	93
2014	1:2000 Rural master plans	Falavarjan Municipality	2014	570	89	95

Table 3
Descriptive information derived from satellite image processing for delineating built-up areas in Falavarjan Township.

Year	Landsat sensor	Total area in hectare	Number of built-up patches
2002	ETM+	2651.7	336
2010	TM	3143.8	317
2014	OLI	4012.2	308

visual interpretation, built-up lands have been substantially expanded, accounting for 113 ha per year. Moreover, LST map has been successfully retrieved by employing the recommended procedure by [Weng et al. \(2004\)](#) (Fig. 3d). LST accuracy assessment was performed through LST ground-trusting points from 3 weather stations. The results are shown in [Table 4](#).

3.2. Analysing statistical relationship between LST values and area of built-up structures

[Fig. 4](#) demonstrates various types of relationships between LST values and area of built-up clusters. As shown in [Tables 5 and 6](#), logarithmic regression yielded the highest value for R^2 (0.35). The area values of built-up structures vary between 0.09 and 398.7 ha in which majority of urban patches areas range between 1 and 60 ha.

Table 4
Accuracy assessment results for land surface temperature generated map in this study.

Weather station		Temperature		Difference
Weather station name	Coordination (lat-lon)	Reference LST	Retrieval LST	
Zefreh	32.501°–51.495°	34.3	32.8	1.5
Sohro-Firoozan	32.493°–51.418°	33.1	32.0	0.9
Poulad-shahr	32.455°–51.534°	38.2	40.1	1.9

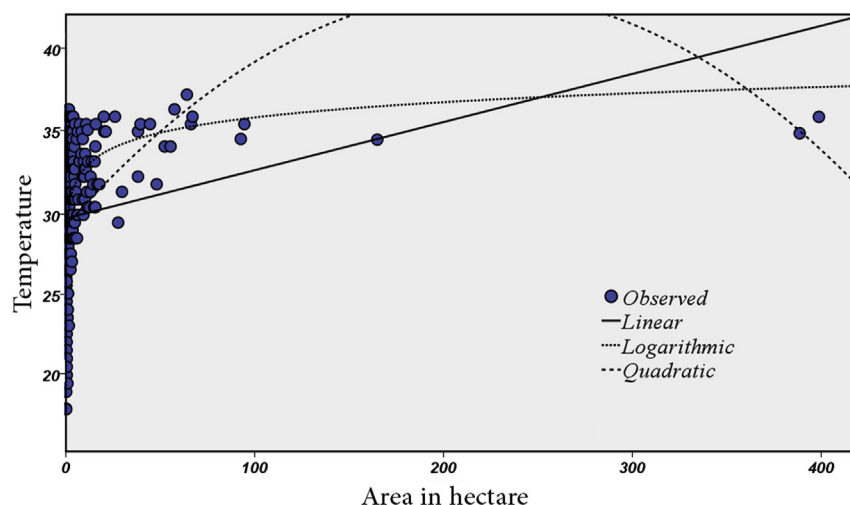


Fig. 4. Various types of relationships between mean LST and area of built-up patches.

Table 5
Coefficient of determination (R square) between land surface temperature values and built-up areas in different regression models.

Statistics	Regression		
	Linear	Quadratic	Logarithmic
Multiple R	0.254	0.133	0.596
R square	0.064	0.0172	0.357
Adjusted R square	0.061	0.0144	0.351
Standard error	3.732	3.826	3.091

Table 6
ANOVA results derived from multiple regression analysis between land surface temperature values and built-up areas.

Regression		df	SS	MS	F	Significance F
Linear	Regression	1	321.6	321.65	23.08	2.34E-06
	Residual	334	4653.3	13.93		
	Total	335	4974.9			
Quadratic	Regression	1	88.7	88.74	6.065	0.014
	Residual	334	4886.2	14.62		
	Total	335	4974.9			
Logarithmic	Regression	1	1768.5	1768.50	184.21	1.01E-33
	Residual	334	3206.4	9.60		
	Total	335	4974.9			

Table 7

Temporal performance evaluation of results derived from logarithmic regression model between land surface temperature values and built-up areas of 20 urban centres in Isfahan province.

year	Mean Area (ha)	Mean LST (Std.)	logarithmic reg. parameters				t-test results		
			constant	b1	R square	Sig.	t	df	Sig.(2-tailed)
2002	104.3	33.04 (0.92)	30.11	1.021	0.48	0.03 ^a	1.82	36	0.075 ^b
2014	128.6	34.75 (0.82)	30.37	0.888	0.49	0.03 ^a			

^a Correlation significant at 0.95 probability.

^b Correlation significant at 0.90 probability.

Having the logarithmic regression model developed for the year 2002, we further investigated whether LST values distribution can be successfully predicted over temporal scales. In doing so, the relationship between mean LST values and the area of 20 built-up patches for 2002 and 2014 were modeled which followed a significant logarithmic regression model (Table 7). The slopes of the two regression models were then compared using *t*-test analysis to determine whether the regression model parameters are statistically stable in a time span of 12 years. The *t*-test results with a threshold of 0.1 are provided in Table 7 suggesting that the two regression models' parameters are not significantly different over years and subsequently can be implemented to explain temporal variations of LST values. Hence, due to the significant similarities between the slope of the two regression curves (Table 7), the logarithmic regression model in 2002 (Table 6) was employed to generate future LST values of predicted urban extents under three growth scenarios (HG, EG and RD).

3.3. Scenario-based urban growth modeling

Fig. 5 illustrates urbanization suitability maps produced in this study to introduce three scenarios of HG, EG and RD to CA-Markov

model. These layers are generated by modifying the weight of factor maps which subsequently influenced the distribution of suitability values. Spatial distribution of suitability values under these patterns can result in different urban growth allocation behaviour for the CA-Markov model in which each growth phenomenon has its own temporal signatures and its specific influence of LST values in Falavarjan Township area.

CA-Markov model was calibrated using 2002 and 2010 land-use layers. The performance of the model was evaluated by simulating the 2014 map layer by which 2010 land-use map was used as the beginning seed year (Dezhkam, Amiri, Darvishsefat, & Sakieh, 2016). According to Table 8, performance evaluation metrics indicate that the model is properly calibrated and can be implemented in the prediction stage (Jafarnezhad, Salmanmahiny, & Sakieh, 2015). The model was executed for three scenarios and three node years were predicted for each scenario (2020, 2025 and 2030, Fig. 6).

3.4. Coupling dynamic urban growth profiles with predictive LST values

Having predictive urban extents of the years 2020, 2025 and

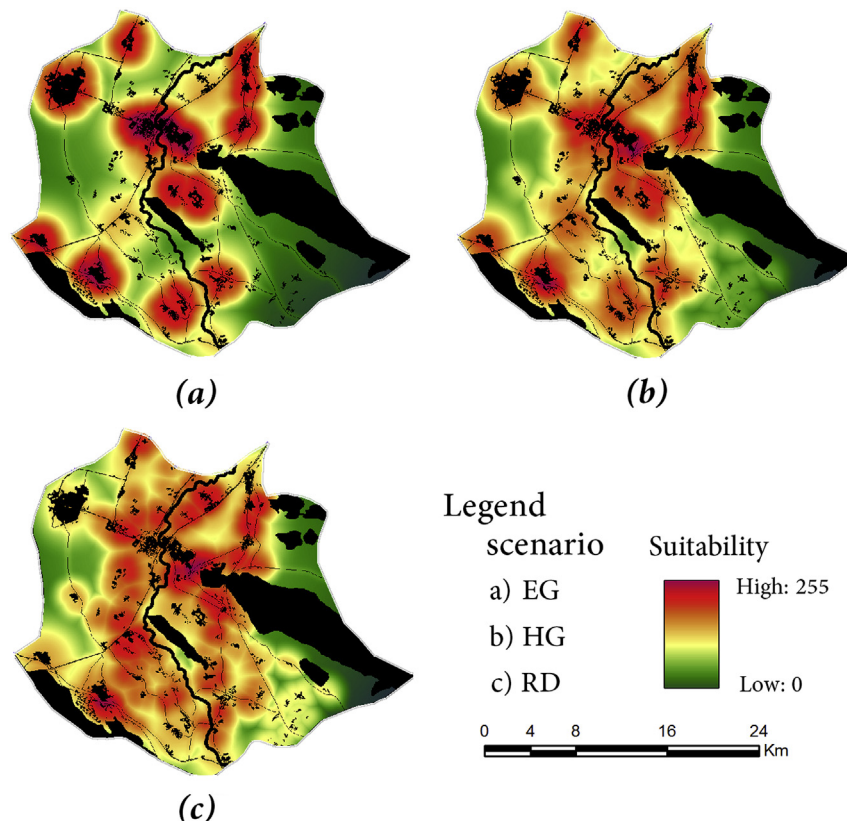


Fig. 5. Urbanization suitability maps related to EG, HG and RD scenarios.

Table 8
CA-Markov chain model validation results.

	Structure based metrics		Pattern based (landscape) metrics		
	ROC	Kappa	Number of patches	Shape index	ENN
Reference map	0.69	0.89	336	0.048	0.35
Simulated map			235	0.071	0.39

2030 generated under predictive scenarios, the area of each built-up patch was entered into the logarithmic regression model to predict its LST value (Fig. 7). The temperature value of 40 °C was considered as a threshold and number of urban patches with LST values above this level for each scenario was counted. According to Table 9, the RD scenario is a more successful policy compared to other growth storylines. According to this scenario, number of cities with LST values above 40 °C, is lower for each node year, which indicates that urban patches of medium physical size with low connectivity pattern are more correlated with lower LST values.

4. Discussion

This study integrated several modeling tools to address the effect of different spatial planning strategies on LST values distribution in a developing region. Hence, the statistical relationship between mean LST and area of built-up patches in 2002, as the central premise of this study, has been used to predict and interpret the future changes in LST pattern under different urban growth policies. In curve estimation, the most significant regression model

was fitted to logarithmic form which is mainly due to the local characteristics of Falavarjan Township area-several urban patches of various physical sizes do exist and are experiencing different periods of their growth cycles. Moreover, temporal validation process was performed to validate the predictive ability of the proposed regression model over time. In this study, the significance of the temporal validation process ($t(36) = 1.82$, $p = 0.075$) is mainly related to the irrigated agricultural landscape in the entire study area which has been resulted a unique local climate. However, it should be noted as the main limitation of this work that the predictive ability of the regression model is not completely satisfied and it must be more accurately validated.

Three urban growth policies in the study area namely historical growth, extensive growth and rural development were also simulated using CA-Markov model to explore how various spatial planning strategies would affect the UHI phenomenon. Based on the results, urban landscape under the RD scenario becomes heavily fragmented and newly urban patches are allocated in a decentralized manner. The built-up structures under this scenario are less connected since they were newly allowed to emerge. According to Sakieh et al. (2015), this planning paradigm is referred to as decentralized urban land-use planning which urban patches are of smaller size are dispersed across the entire landscape. In contrast, urban patches under EG scenario experience a linear and outward expansion and coalescence of built-up clusters would result in a series of main urban cores that might possess high LST values (exceeding the mean LST of 8 cities to more than 40 °C in 2030). Although the RD scenario yielded better results in terms of LST values, the HG scenario outputs are very close to those of derived from the RD alternative. From the standpoint of a policy

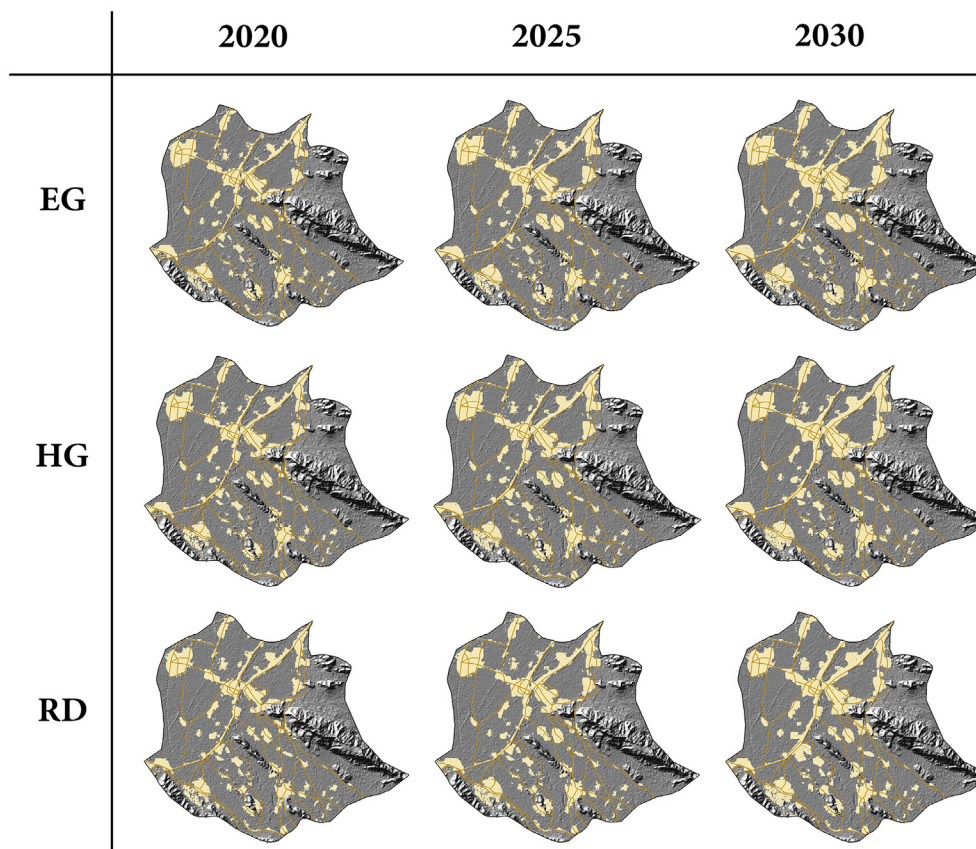


Fig. 6. Simulated future urban growth maps of the study area under EG, HG and RD scenarios.

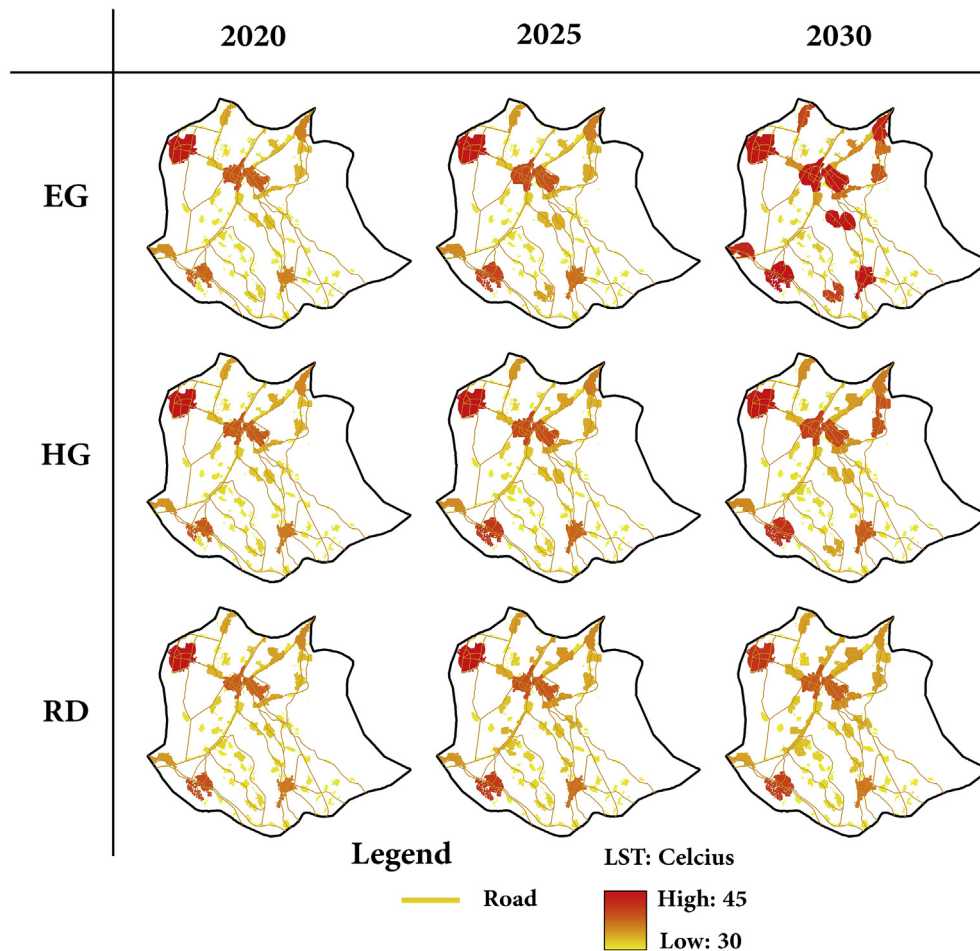


Fig. 7. Geographical distribution of the predicted mean LST values related to each urban growth scenarios in 2020, 2025, and 2030.

Table 9

Comparing three predictive scenarios of HG (historical growth), EG (extensive growth) and rural development (RD) for their effect on land surface temperature in interior urban environments.

	RD scenario (2020–25–30)	HG scenario (2020–25–30)	EG scenario (2020–25–30)
Mean land surface temperature	37.7–38.0–38.1	37.7–37.9–38.0	37.6–37.8–38.0
Cities with land surface temperature more than 40 °C	1–2–3	1–3–4	2–5–8

maker, this scenario might be a compromised and more preferable solution. Because historical growth patterns are the most probable scenarios to happen, and therefore they are simpler to understand and are desired by policy makers and authorities. Considering the abovementioned items, it can be stated that a realistic and practical growth scenario would allow historical growth profile to occur, but the spatial pattern should be regulated in terms of sustainability criteria discussed in this paper.

Overall, building a new countryside under a decentralized pattern is a recommended policy in central Iran. The EG alternative projected the likely large amount of land resources loss, which is associated with increased LST values. Spontaneous growth of rural areas is allowed to occur but their physical size should be monitored to prevent the unpleasant effects of LST phenomenon on citizens' health. Thus, establishment of a decentralized rural land development plan is a proven and applicable way that can contribute to an urban landscape with lower levels of environmental consequences such as UHI. This is an applicable strategy in a

developing region in Iran since population growth rate is still high and lack of regional planning regulations cause the landscape to be occupied with the same amount and pattern of growth as its historical profile. However, the morphology of allocated urban patches can be regulated in terms of lower LST consideration.

5. Conclusions

In this study, the main attention is paid to the predictive ability of LST and its application in terms of adopting optimized strategies for an integrated urban-rural land development system. Such comparative and scenario-based studies can quantify and visualize the interactions between climatic parameters and land surface processes, which finally shed insights on designing sustainable urban landscapes. The findings of this study not only provide an informed set of solutions for implementation of building a new countryside strategy in central Iran, but also new approaches for integrated urban-rural planning efforts in a rapidly developing

region.

Although the proposed approach is conceptually simple and also has limitations, especially in temporal validation process, it could be considered as the first attempt to evaluate the predictive ability of LST and its association with sustainable planning. Finally, our suggestions that remains open for future research corresponds to:

- 1) Evaluating different types of regression models, especially non-linear relations, to raise the knowledge of the variability and the behaviour of LST in relation to different size and types of land-use/covers;
- 2) Fitting the regression models by utilizing other independent variables (spatial and non-spatial), such as configuration and structure of land-use/cover types and climatic parameters;
- 3) Evaluating temporal predictive ability of LST under different conditions such as comparison of more than two regression models, determining the timespan at which the LST becomes non-predictive, and applying a combination of in-situ and air-borne LST variable data for temporal validation process; and
- 4) Applying the predictive ability of LST in sustainable land-use planning efforts such as identifying optimal urban growth trajectories at different scales and implementing an improved land-use allocation system by considering probable future changes in thermal conditions.

Conflict of interest

The authors declare that they have no conflict of interest.

References

- Alhowaish, A. K. (2015). Eighty years of urban growth and socioeconomic trends in Dammam Metropolitan Area, Saudi Arabia. *Habitat International*, 50, 90–98.
- Amiri, R., Weng, Q., Alimohammadi, A., & Alavipanah, S. (2009). Spatial-temporal dynamics of land surface temperature in relation to fractional vegetation cover and land use/cover in the Tabriz urban area, Iran. *Remote Sensing of Environment*, 113, 2606–2617.
- Aronoff, S. (2005). *Remote sensing for GIS managers*. New York: Esri Press.
- Asgarian, A., Amiri, B. J., & Sakieh, Y. (2014). Assessing the effect of green cover spatial patterns on urban land surface temperature using landscape metrics approach. *Urban Ecosystems*, 18, 209–222.
- Bokaei, M., Zarkesh, M. K., Arasteh, P., & Hosseini, A. (2016). Assessment of urban heat island based on the relationship between land surface temperature and land use/land cover in Tehran. *Sustainable Cities and Society*, 35, 94–104.
- Bryan, B. A., Crossman, N. D., King, D., & Meyer, W. S. (2011). Landscape futures analysis: assessing the impacts of environmental targets under alternative spatial policy options and future scenarios. *Environmental Modelling & Software*, 26, 83–91.
- Chaudhuri, G., & Mishra, N. B. (2016). Spatio-temporal dynamics of land cover and land surface temperature in Ganges-Brahmaputra delta: a comparative analysis between India and Bangladesh. *Applied Geography*, 68, 68–83.
- Dezhkam, S., Amiri, B. J., Darvishsefat, A. A., & Sakieh, Y. (2016). Performance evaluation of land change simulation models using landscape metrics. *Geocarto International*. <http://dx.doi.org/10.1080/10106049.2016.1167967>.
- Douglas, I., Goode, D., Houck, M., & Wang, R. (2011). *The Routledge handbook of urban ecology*. Oxon and New York: Routledge Abingdon.
- Du, S., Xiong, Z., Wang, Y. C., & Guo, L. (2016). Quantifying the multilevel effects of landscape composition and configuration on land surface temperature. *Remote Sensing of Environment*, 178, 84–92.
- Eastman, R. (2009). *Idrisi Taiga version. 16.01 Clark laboratories*. Worcester, MA: Clark University.
- Feng, X., & Myint, S. W. (2016). Exploring the effect of neighboring land cover pattern on land surface temperature of central building objects. *Building and Environment*, 95, 346–354.
- Feng, H., Zhao, X., Chen, F., & Wu, L. (2014). Using land use change trajectories to quantify the effects of urbanization on urban heat island. *Advances in Space Research*, 53, 463–473.
- FMS. (2002). *Investigating the impact of urban environment on health condition in Isfahan*. Isfahan University. Medical department, 168.
- Goodarzi, M. S., Sakieh, Y., & Navardi, S. (2016). Scenario-based urban growth allocation in a rapidly developing area: a modeling approach for sustainability analysis of an urban-coastal coupled system. *Environment, Development and Sustainability*. <http://dx.doi.org/10.1007/s10668-016-9784-9>.
- Gu, C. L., Hu, L. Q., Zhang, X. M., Wang, X. D., & Guo, J. (2011). Climate change and urbanization in the Yangtze river delta. *Habitat International*, 35, 544–552.
- Hansen, H. S. (2010). Modelling the future coastal zone urban development as implied by the IPCC SRES and assessing the impact from sea level rise. *Landscape and Urban Planning*, 98, 141–149.
- He, C., Zhao, Y., Huang, Q., Zhang, Q., & Zhang, D. (2015). Alternative future analysis for assessing the potential impact of climate change on urban landscape dynamics. *Science of The Total Environment*, 532, 48–60.
- Huang, C., Chen, W., Li, Y., Shen, H., & Li, X. (2016). Assimilating multi-source data into land surface model to simultaneously improve estimations of soil moisture, soil temperature, and surface turbulent fluxes in irrigated fields. *Agricultural and Forest Meteorology*. <http://dx.doi.org/10.1016/j.agrformet.2016.03.013> (in press).
- Isfahan Municipality. (2016). *Sustainable development sector data archive*. no: 5054992.
- Jafarnezhad, J., Salmanmahiny, A., & Sakieh, Y. (2015). Subjectivity versus objectivity: comparative study between Brute force method and Genetic algorithm for calibrating the SLEUTH urban growth model. *Urban Planning and Development*. [http://dx.doi.org/10.1061/\(ASCE\)UP.1943-5444.0000307](http://dx.doi.org/10.1061/(ASCE)UP.1943-5444.0000307).
- Jusuf, S. K., Wong, N. H., Hagen, E., Anggoro, R., & Hong, Y. (2007). The influence of land use on the urban heat island in Singapore. *Habitat International*, 31(2), 232–242.
- Lu, D., & Weng, Q. (2005). Urban classification using full spectral information of Landsat ETM+ imagery in Marion County, Indiana. *Photogrammetric Engineering & Remote Sensing*, 71, 1275–1284.
- Niemelä, J., Breuste, J. H., Guntenspergen, G., McIntyre, N. E., Elmqvist, T., & James, P. (2011). *Urban ecology: Patterns, processes, and applications*. Oxford University Press.
- Saaty, T. L. (1990). *The analytic hierarchy process: Planning, priority setting, resource allocation*.
- Sakieh, Y., Amiri, B. J., Danekar, A., Feghhi, J., & Dezhkam, S. (2014a). Scenario-based evaluation of urban development sustainability: an integrative modeling approach to compromise between urbanization suitability index and landscape pattern. *Environment, Development and Sustainability*, 1–23.
- Sakieh, Y., Amiri, B. J., Danekar, A., Feghhi, J., & Dezhkam, S. (2014b). Simulating urban expansion and scenario prediction using a cellular automata urban growth model, SLEUTH, through a case study of Karaj City, Iran. *Journal of Housing and the Built Environment*, 1–21.
- Sakieh, Y., & Salmanmahiny, A. (2016). Treating a cancerous landscape: implications from medical sciences for urban and landscape planning in a developing region. *Habitat International*. <http://dx.doi.org/10.1016/j.habitatint.2016.03.008>.
- Sakieh, Y., Salmanmahiny, A., Jafarnezhad, J., Mehri, A., Kamyab, M., & Galdavi, S. (2015). Evaluating the strategy of decentralized urban land-use planning in a developing region. *Land Use Policy*, 48, 534–551.
- Sánchez-Rodríguez, R. (2005). *Science plan: Urbanization and global environmental change*. International Human Dimensions Programme on Global Environmental Change.
- Schneider, A., Friedl, M. A., & Potere, D. (2010). Mapping global urban areas using MODIS 500-m data: new methods and datasets based on 'urban ecoregions'. *Remote Sensing of Environment*, 114, 1733–1746.
- Sobrino, J. A., Jiménez-Muñoz, J. C., & Paolini, L. (2004). Land surface temperature retrieval from LANDSAT TM 5. *Remote Sensing of Environment*, 90, 434–440.
- Solomon, S. (2007). *Climate change 2007-the physical science basis: Working group I contribution to the fourth assessment report of the IPCC*. Cambridge University Press.
- Tan, M., & Li, X. (2015). Quantifying the effects of settlement size on urban heat islands in fairly uniform geographic areas. *Habitat International*, 49, 100–106.
- Verborg, P. H., van Berkel, D. B., van Doorn, A. M., van Eupen, M., & van den Heiligenberg, H. (2010). Trajectories of land use change in Europe: a model-based exploration of rural futures. *Landscape Ecology*, 25, 217–232.
- Vlassova, L., & Pérez-Cabello. (2016). Effects of post-fire wood management strategies on vegetation recovery and land surface temperature (LST) estimated from Landsat images. *International Journal of Applied Earth Observation and Geoinformation*, 44, 171–183.
- Weng, Q., Lu, D., & Schubring, J. (2004). Estimation of land surface temperature-vegetation abundance relationship for urban heat island studies. *Remote Sensing of Environment*, 89, 467–483.
- Wu, J. (2010). Urban sustainability: an inevitable goal of landscape research. *Landscape Ecology*, 25, 1–4.
- Wu, J. (2014). Urban ecology and sustainability: the state-of-the-science and future directions. *Landscape and Urban Planning*, 125, 209–221.
- Wu, J., & Wu, T. (2013). *Ecological resilience as a foundation for urban design and sustainability. Resilience in Ecology and Urban Design* (pp. 211–229). Springer.
- Xiang, W. N., & Clarke, K. C. (2003). The use of scenarios in land-use planning. *Environment and Planning B*, 30, 885–909.
- Zadeh, L. A. (1965). Fuzzy sets. *Information and control*, 8, 338–353.
- Zhou, W., Huang, G., & Cadenasso, M. L. (2011). Does spatial configuration matter? Understanding the effects of land cover pattern on land surface temperature in urban landscapes. *Landscape and Urban Planning*, 102, 54–63.
- Zhou, B., Rybski, D., & Kropp, J. P. (2013). On the statistics of urban heat island intensity. *Geophysical Research Letters*, 40, 5486–5491.